Detailed analysis of the PNJL phase diagram

Critical properties within an effective model of QCD

Hubert Hansen <hansen@ipnl.in2p3.fr>

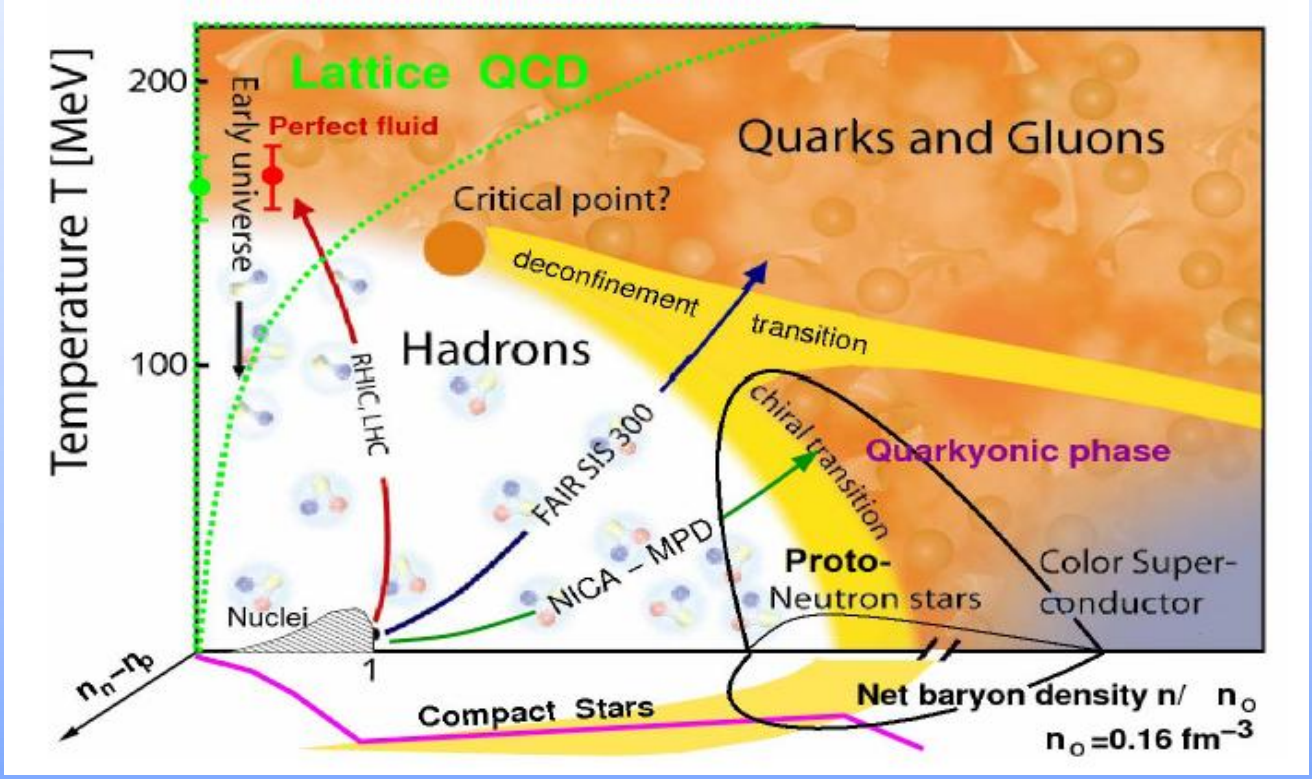

Institut de Physique Nucléaire de Lyon, CNRS/IN2P3 and université Claude Bernard de Lyon
Collaborators: A. Gatti, G. Chanfray, G. Goessens, P. Costa, M. Ruivo, C. Da Sousa

Part I: Phases of QCD, symmetries and effective models

Lagrangian of QCD: $\mathcal{L}_{QCD} = \bar{q}\,(\,i\gamma^\mu D_\mu - \hat{m}\,)\,q - \frac{1}{4}F^a_{\mu\nu}\,F^{\mu\nu}_a$

$q = (u, d, s, c, b, t)$; $N_c = 3$; $\hat{m} = \mathrm{diag}_f(m_u, m_d, \ldots)$; $D_\mu = \partial_\mu - igt^a\,A^a_\mu$ with A^a_μ $(a = 1, 2, ..., 8)$ the gauge field and $F_{\mu\nu}$ the gluon field strength tensor.

$\Rightarrow$ Symmetric under SU(3) gauge transformations in color space

Low energy: Relevant to the study of hadronic properties.
Non-perturbative structure: existence of quark condensates $\langle\bar{q}q\rangle$, appearance of light pseudoscalar particles ((quasi) Goldstone bosons). Confinement of quarks.

Group of symmetries for $N_f = 3$ in the chiral limit $m_u = m_d = m_s = 0$:
$\rightarrow$ $\mathrm{SU}_V(3)$ and $\mathrm{U}_V(1)$: conservation of isospin and baryon number ;
$\rightarrow$ $\mathrm{SU}_A(3)$ and $\mathrm{U}_A(1)$ (chiral and axial symmetry): alter the parity.

$$\mathrm{U}(3)_L \otimes \mathrm{U}(3)_R = \mathrm{SU}_V(3) \otimes \mathrm{SU}_A(3) \otimes \mathrm{U}_V(1) \otimes \mathrm{U}_A(1).$$

Symmetry	Transformation	Current	Name	Manifestation in nature
$\mathrm{SU}_V(3)$	$q \rightarrow \exp(-i\frac{\lambda_a\alpha_a}{2})q$	$V^a_\mu = \bar{q}\gamma_\mu\frac{\lambda_a}{2}q$	Isospin	Approximately conserved
$\mathrm{U}_V(1)$	$q \rightarrow \exp(-i\alpha_V)q$	$V_\mu = \bar{q}\gamma_\mu q$	Baryonic	Conserved
$\mathrm{SU}_A(3)$	$q \rightarrow \exp(-i\frac{\gamma_5\lambda_a\theta_a}{2})q$	$A^a_\mu = \bar{q}\gamma_\mu\gamma_5\frac{\lambda_a}{2}q$	Chiral	Spontaneously broken
$\mathrm{U}_A(1)$	$q \rightarrow \exp(-i\gamma_5\alpha_A)q$	$A_\mu = \bar{q}\gamma_\mu\gamma_5 q$	Axial	" $\mathrm{U}_A(1)$ problem"

Hadronic spectrum: chiral and axial symmetry breaking

Wigner realization of chiral and axial symmetries:

existence of multiplet of particles with same mass and opposite parity for each multiplet of isospin (chiral partners)

$U_A(1) \Rightarrow$ partner with opposite parity to each hadron

False experimentally in the hadronic spectrum (low energy)

Spontaneous chiral symmetry breaking: Goldstone phase

$SU_A(3)$ symmetry: mechanism for the *spontaneous breaking of chiral symmetry*, related to the existence of non-zero quark condensates, $\langle \bar{q}q \rangle$ (not invariant under $SU_A(3)$) ; they act as as order parameters for the spontaneously broken chiral symmetry phase.

Goldstone theorem: existence of eight degenerate Goldstone bosons e.g. pions ($M_\pi/M_N = 0.15$).

Lifting of the degeneracy in the pseudoscalar mesons spectrum: explicit symmetry breaking due to current quark masses m_u, m_d and m_s.

Case of the $\eta - \eta'$

Classically, massless QCD possesses the $U_L(3) \times U_R(3)$ symmetry but η' not of the Goldstone type $\Rightarrow$ Adler–Jackiw–Bell $U_A(1)$ anomaly (whose origin is instantons) breaks this symmetry to $SU_L(3) \times SU_R(3)$ (large mass for the η')

$\Rightarrow$ **Finally:** QCD as (almost) $SU_L(3) \times SU_R(3)$ chiral symmetry ; at low energy, the pertinent degrees of freedom are mesons (QCD experiences a confined/deconfined phase transition) ; mesons give insight on the non-perturbative vacuum.

QCD Phase Diagram

Characteristics of the transition well established for $\mu_B = 0$:
Rapid increase of energy density (and other thermodynamic quantities) $\Rightarrow$ transition from hadronic resonance gas to a matter of deconfined quarks and gluons (the rise is interpreted as the liberation of many degrees of freedom) with the Polyakov loop as order parameter.

Finite temperature and chemical potential: in most three-flavor phase diagram it exists a CEP (critical end point) that ends a first–order chiral phase transition (separating hadronic and quark phases) that starts at $\mu \neq 0$ and $T = 0$ (becomes a tricritical point – TCP – in the chiral limit).

From the experimental point of view:

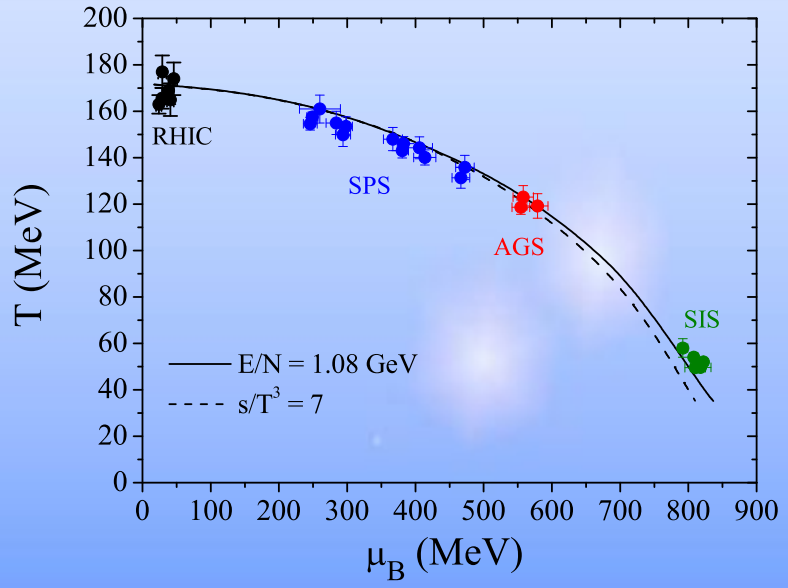

Freeze-out points for the different beam energies are showed, Cleymans, Oeschler, Redlich and Wheaton, Phys. Rev. C73, 034905 (2006).

$U_A(1)$ symmetry breaking and effective t'Hooft interaction

If $U_A(1)$ symmetry spontaneously broken: pseudoscalar Goldstone boson with mass $\sqrt{3}M_\pi$ (Weinberg). Candidates with the correct quantum numbers: $\eta(549)$ identified as belonging to the octet of pseudoscalar mesons and $\eta'(985) \simeq M_{Nucleon}$ (mass too high: "η' problem")

$\Rightarrow$ If a particle with the characteristics pointed out by Weinberg does not exist, then where is the ninth Goldstone boson ?

$\Rightarrow$ If this Goldstone boson does not exist there is no spontaneous breaking of $U_A(1)$ symmetry.

1976 (G. 't Hooft): $U_A(1)$ symmetry does not exist at the quantum level (explicitly broken by the axial anomaly described at the semiclassical level by instantons). Instantons "transform" left handed fermions into right handed ones and conversely with non zero axial charge variation: $\Delta Q_5 = \pm 2N_f$

"'t Hooft determinant" mimics this interaction in a purely fermionic effective theory ("absorbs" N_f left helicity fermions and convert them):

$$\mathcal{L}_{inst} = g_D e^{i\theta_{inst}} \det_{flavor} (\bar{q}_R(x) q_L(x)) + h.c.$$

$\Rightarrow$ Explicit breaking of $U_A(1)$ symmetry: η' about 1 GeV (the mass of η' has a different origin than the other masses of the pseudoscalar mesons ; not the missing Goldstone boson)

$U_A(1)$ anomaly responsible for the flavor mixing effect that removes the degeneracy among several mesons.

$\Rightarrow$ Finally, an interesting question also related to these symmetries is whether both chiral $SU(N_f)\times SU(N_f)$ and axial $U_A(1)$ symmetries are restored in the high temperature/density phase and which observables could carry information about these restorations.

Nambu-Jona-Lasinio effective models of QCD

Motivated by chiral symmetry (Ginzburg-Landau theory) ; used as reference when one add Z_{N_c}.

Extended NJL Lagrangian: $\boxed{\mathcal{L}_{NJL} = \mathcal{L}_0 + \mathcal{L}_4 + \mathcal{L}_6}$ with

$$\begin{aligned}
\mathcal{L}_0 &= \bar{q}(i\gamma^\mu \partial_\mu - \hat{m}_0)q \\
\mathcal{L}_4 &= G_1 \left[(\bar{q}\lambda_a q)^2 + (\bar{q} i\gamma_5 \lambda_a q)^2 \right] \\
\mathcal{L}_6 &= g_D(\det_{flavor} \bar{q} P_L q + \det_{flavor} \bar{q} P_R q)
\end{aligned}$$

$\bar{q} = (\bar{u}, \bar{d}, \bar{s})$, $\hat{m} = diag(m_u, m_d, m_s)$, $P_{L,R} = \frac{1 \mp \gamma_5}{2}$; $\lambda_{a, a\in[0,8]}$: Gell–Mann matrices (flavor).

- Invariant under global color symmetry $SU(N_c)$
- 4-quarks interaction: $\mathcal{L}_4$ has $U_L(3) \times U_R(3)$ chiral symmetry (in QCD 4-quarks interactions exist via exchange of gluons ; G_1 mimicks a frozen gluon propagator leading to a contact interaction)
- $\mathcal{L}_6 \Rightarrow U_A(1)$ anomaly breaks $U_L(3) \times U_R(3)$ to $U_V(1) \times SU_L(3) \times SU_R(3)$
- $\hat{m}_0 \Rightarrow$ explicit chiral symmetry breaking term: $SU_L(3) \times SU_R(3) \Rightarrow SU_V(3)$ if $m_u = m_d = m_s$. When $m_0 \neq 0$ the chiral symmetry is broken. But small breaking ($m_0 << \Lambda_{QCD}$): does not explain differences between chiral partner.

The Polyakov Loop and the $\mathbb{Z}_3$ Symmetry Breaking: Pure Gauge

Polyakov loop in imaginary time and Polyakov gauge $A_\mu = \delta_{\mu 4} A_4$

$L(\vec{x}) = \mathcal{P} \exp\left[i \int_0^\beta d\tau \, A_4(\vec{x}, \tau) \right]$ $\Rightarrow$ **effective field** $\Phi = \frac{1}{N_c} Tr_C \, L$

$A_4 = iA^0$: temporal component of the Euclidean gauge field $(\vec{A}, A_4)$, $\beta = 1/T$, $\mathcal{P}$: path ordering.

L transports the field A_μ from the point in space-time $(\vec{x}, 0)$ to $(\vec{x}, \beta)$

$\Rightarrow$ $\Phi = 0$ means confinement ; $\Phi = 1$ means free propagation (deconfinement)

Effective potential $\mathcal{U}(\Phi, \bar{\Phi}; T)$: $T_0 = 270$ MeV

$$\frac{\mathcal{U}(\Phi, \bar{\Phi}; T)}{T^4} = -\frac{a(T)}{2}\bar{\Phi}\Phi + b(T)\ln[1 - 6\bar{\Phi}\Phi + 4(\bar{\Phi}^3 + \Phi^3) - 3(\bar{\Phi}\Phi)^2]$$

where $a(T) = a_0 + a_1 \left(\frac{T_0}{T}\right) + a_2 \left(\frac{T_0}{T}\right)^2$

and $b(T) = b_3 \left(\frac{T_0}{T}\right)^3$

a_0	a_1	a_2	b_3
3.51	-2.47	15.2	-1.75

Table 1: Parameters for the effective potential in the pure gauge sector.

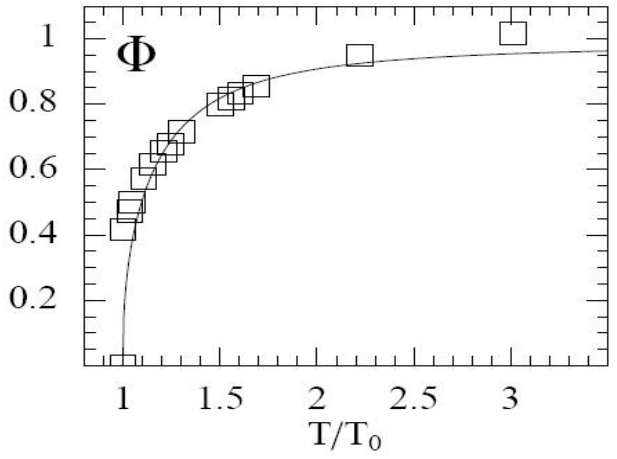

C. Ratti, M. Thaler, W.Weise, hep-ph/0604025 : lattice: O. Kaczmarek, F. Karsch, P. Petreczky, F. Zantow, Phys. Lett. B **543**, 41 (2002).

Polyakov – Nambu – Jona-Lasinio effective model

$$\mathcal{L}_{PNJL} = \bar{q}(i\gamma_\mu D^\mu - \hat{m})q$$
$$+ \frac{1}{2} g_S \sum_{a=0}^{8} [(\bar{q}\lambda^a q)^2 + (\bar{q} i\gamma_5 \lambda^a q)^2]$$
$$+ g_D\{\det[\bar{q}(1+\gamma_5)q] + \det[\bar{q}(1-\gamma_5)q]\}$$
$$- \mathcal{U}\left(\Phi[A], \bar{\Phi}[A]; T\right) + \mu\bar{q}\gamma_0 q$$

Here $q = (q_u, q_d, q_s)$ are the quark fields, $\hat{m} = \mathrm{diag}(m_u, m_d, m_s)$, λ^a are the flavor $\mathrm{SU}_f(3)$ Gell–Mann matrices ($a = 0, 1, \ldots, 8$), with $\lambda^0 = \sqrt{\frac{2}{3}}\mathbb{I}$ and $D^\mu = \partial^\mu - iA^\mu$

$\mathcal{U}\left(\Phi[A], \bar{\Phi}[A]; T\right)$ acts as a (gluonic) pressure in which quarks propagate.

Order parameters

Spontaneous chiral symmetry breaking: Mean field point of view with $N_f = 2$

if $G_1(\bar{q}q)^2 \simeq 2G_1\langle\bar{q}q\rangle\ \bar{q}q$ then the lagrangian reduces to a free Lagrangian $\bar{q}(i\gamma^\mu\partial_\mu - m)q$ with mass $m = m_0 + 2G_1\langle\bar{q}q\rangle \simeq \Lambda_{QCD}$

$\langle\bar{q}q\rangle \neq 0 \Rightarrow$ spontaneous chiral symmetry breaking

$\langle\bar{q}q\rangle \Rightarrow$ order parameter (similar to magnetisation): tells you in which phase you are.

$\rightarrow < \bar{q}_u q_u > = < \bar{q}_d q_d >$: order parameter for the light sector ($\mathrm{SU}_R(2) \times \mathrm{SU}_L(2)$ chiral symmetry)

$\rightarrow < \bar{q}_s q_s >$: order parameter for the strange sector (topological susceptibility also gives an information)

If no explicit breaking, the phase transition is second order.

Confinement / $\mathbb{Z}_3$ Symmetry Breaking:

$\rightarrow \Phi = 0$: no transport of color charges $\Rightarrow$ confinement

$\rightarrow \Phi = 1$: free "propagation" (parallel transport) of color charges $\Rightarrow$ deconfinement.

If no explicit breaking (pure gauge i.e. $m \rightarrow \infty$), the phase transition is second order.

In QCD there is an explicit breaking of $\mathbb{Z}_3$ symmetry due to the kinetic term. Hence, for large mass (chiral symmetry breaking case) the kinetic term is negligible ($m\bar{\psi}\psi \gg \bar{\psi}i\gamma^\mu D_\mu\psi$) $\Rightarrow$ steep crossover from the restored symmetry zone to the broken symmetry zone.

At the contrary when the mass is small (chiral restoration) the crossover is less steep.

The same effect is observed with high chemical potential: the kinetic term is important due to Fermi motion: $m\bar{\psi}\psi < \bar{\psi}i\partial\!\!\!/\psi + \mu\psi^\dagger\psi \simeq \mu\psi^\dagger\psi$

Mean Field Approximation

Chemical equilibrium condition $\mu_u = \mu_d = \mu_s = \mu$. This choice allows for isospin symmetry, $m_u = m_d$ and approximates the physical conditions at RHIC.

Quark propagator:

The quark propagator in the constant background field A_4 is then:

$$S_i(p) = -(\not{p} - M_i + \gamma_0(\mu - iA_4))^{-1}$$

In the above, $p_0 = i\omega_n$ and $\omega_n = (2n+1)\pi T$ is the Matsubara frequency for a fermion.

Gap equations: constituent quark masses (dynamical masses)

$$\boxed{M_i = m_i - 2g_S \langle \bar{q}_i q_i \rangle - 2g_D \langle \bar{q}_j q_j \rangle \langle \bar{q}_k q_k \rangle}$$

where the quark condensates $\langle \bar{q}_i q_i \rangle$, with $i, j, k = u, d, s$
(to be fixed in cyclic order), have to be determined in a self-consistent way with:

$$\langle \bar{q}_i q_i \rangle = -2N_c \int \frac{\mathrm{d}^3 p}{(2\pi)^3} \frac{M_i}{E_i} [\theta(\Lambda^2 - \vec{p}^2) - f_\Phi^{(+)}(E_i) - f_\Phi^{(-)}(E_i)]$$

where E_i is the quasi-particle energy for the quark i: $E_i = \sqrt{\mathbf{p}^2 + M_i^2}$.

Grand Potential in the Mean Field Approximation

PNJL grand canonical potential density:

$$\Omega(\Phi,\bar{\Phi},M_i;T,\mu)=\mathcal{U}\left(\Phi,\bar{\Phi},T\right)$$
$$+g_S\sum_{\{i=u,d,s\}}\langle\bar{q}_iq_i\rangle^2+4g_D\langle\bar{q}_uq_u\rangle\langle\bar{q}_dq_d\rangle\langle\bar{q}_sq_s\rangle-2N_c\sum_{\{i=u,d,s\}}\int_\Lambda\frac{\mathrm{d}^3p}{(2\pi)^3}E_i$$
$$-2T\sum_{\{i=u,d,s\}}\int\frac{\mathrm{d}^3p}{(2\pi)^3}\left\{\mathrm{Tr}_c\ln\left[1+\boldsymbol{L}\mathrm{e}^{-(E_i-\mu)/T}\right]+\mathrm{Tr}_c\ln\left[1+\boldsymbol{L}^\dagger\mathrm{e}^{-(E_i+\mu)/T}\right]\right\}$$

where E_i is the quasi-particle (Hartree) energy for the quark i: $E_i=\sqrt{\mathbf{p}^2+M_i^2}$

The propagation of the quarks into the medium filled with (background) gluon fields with pressure $\mathcal{U}$ leads to statiscal suppression of 1- and 2-quarks propagation (statiscal confinement) :

$$\mathrm{Tr}_c\ln\left[1+\boldsymbol{L}\mathrm{e}^{-(E_p-\mu)/T}\right]=\ln\left[1+3\boldsymbol{\Phi}e^{-\beta(E_p-\mu)}+3\bar{\boldsymbol{\Phi}}e^{-2\beta(E_p-\mu)}+e^{-3\beta(E_p-\mu)}\right]$$
$$\lim_{\Phi,\bar{\Phi}\to0}(\mathbb{Z}_3\text{ restored})=\ln\left[1+e^{-3\beta(E_p-\mu)}\right]$$
$$\lim_{\Phi,\bar{\Phi}\to1}(\mathbb{Z}_3\text{ broken})=N_c\ln\left[1+e^{-\beta(E_p-\mu)}\right]$$

Part II: Detailed study of the SU(2) case

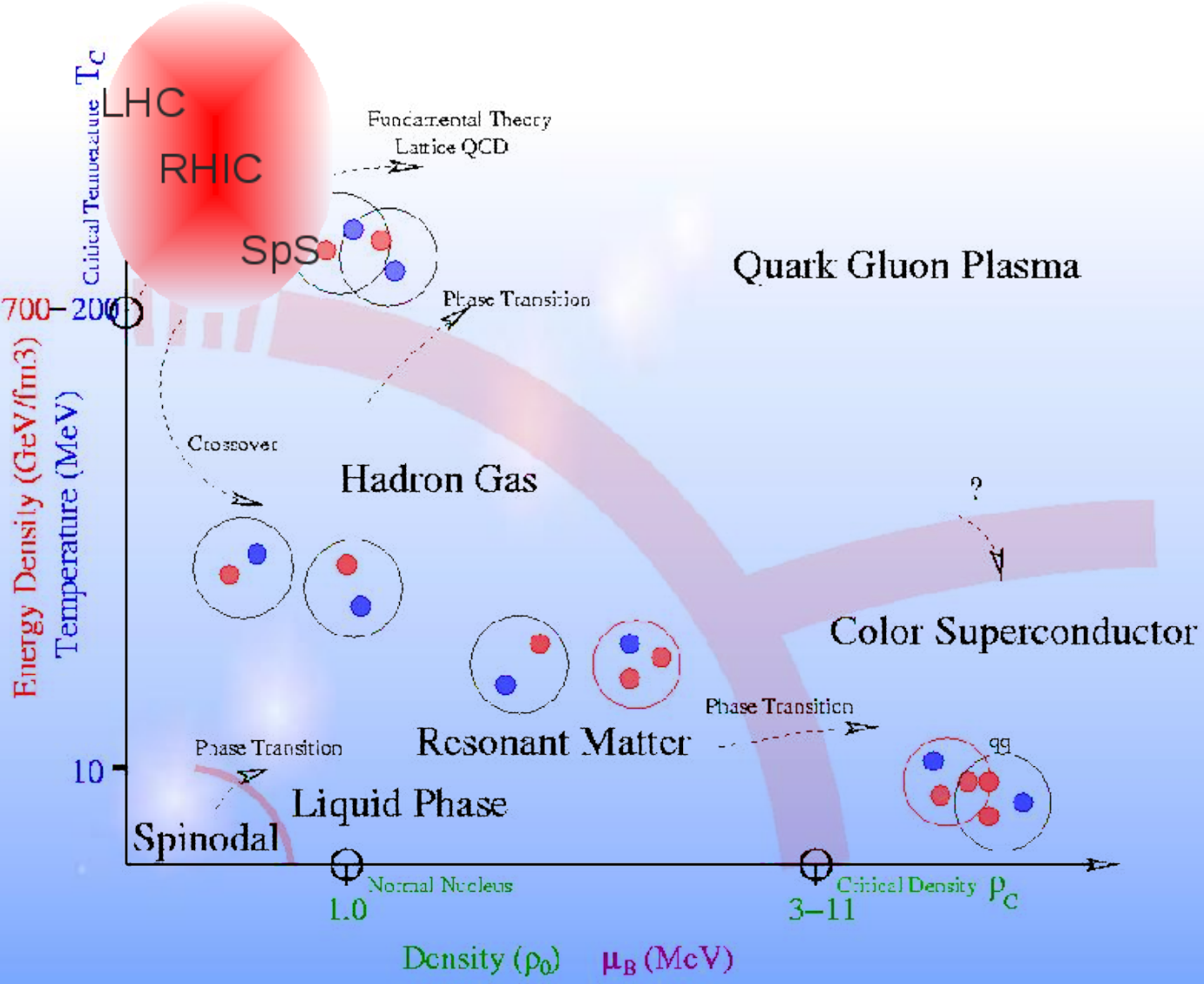

(Yves Schutz)

Chiral condensate and Polyakov loop: crossover vs. 1st order

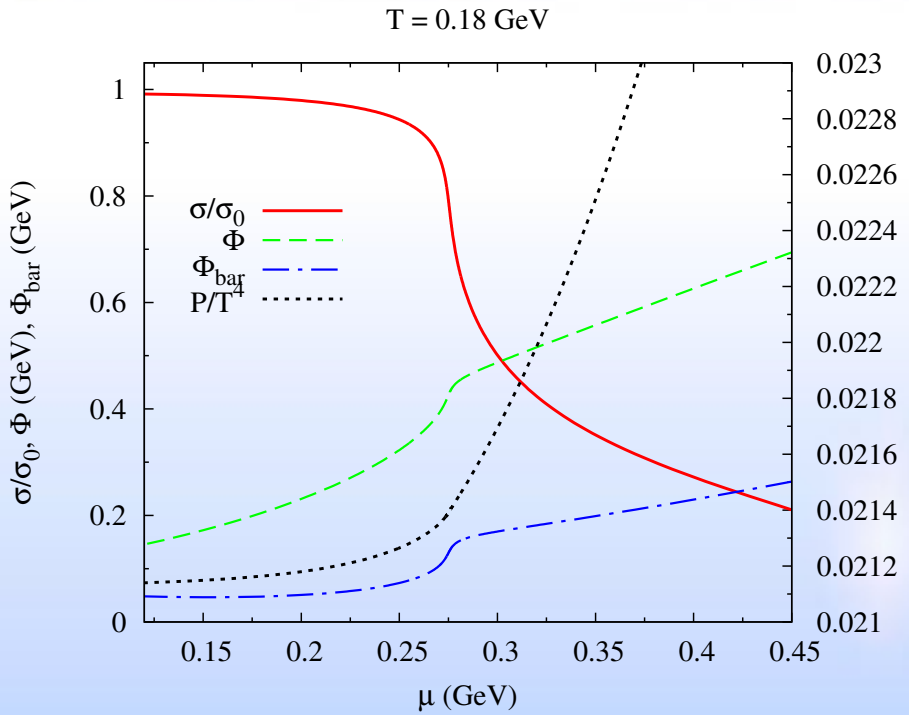

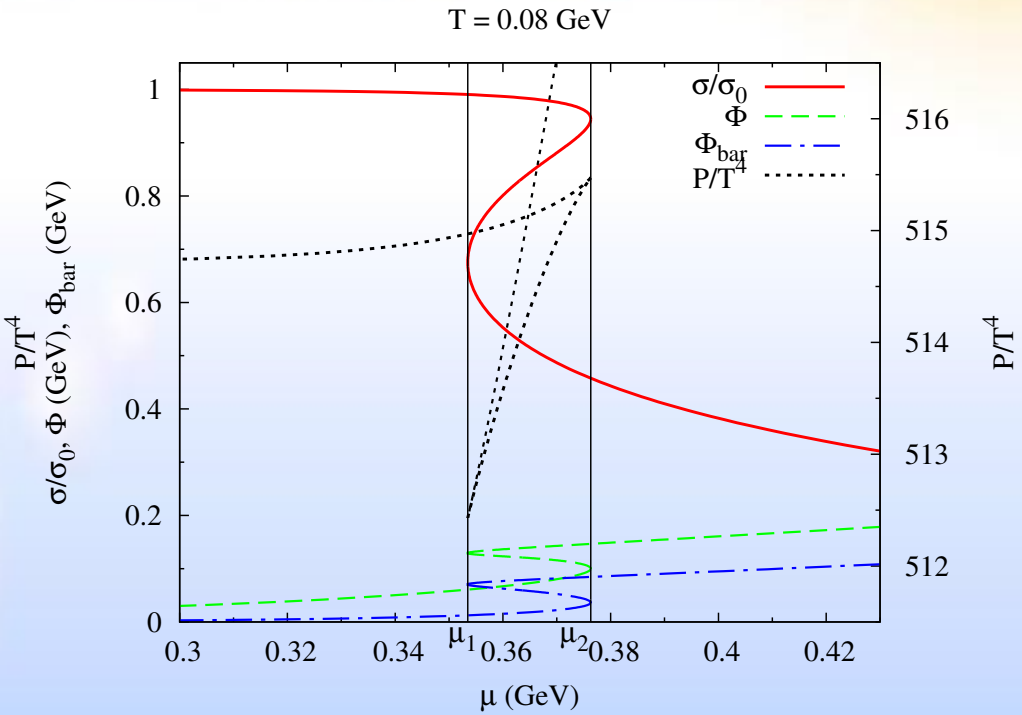

Left: Condensate, Polyakov loop and scaled pressure in the chiral cross over zone; the cross-over value is fixed studying the minimum of $\frac{-dT}{dm}$ at μ set.
Right: Condensate, Polyakov loop and scaled pressure in the first order chiral phase transition zone. The lines μ_1, μ_2 locate the metastable zone, and the intersection point of the grand potential relating to the inferior and to the superior branch of the condensate identify the chemical potential that correspond at the first order transition.

Chiral phase diagram (PNJL): chemical potential and density

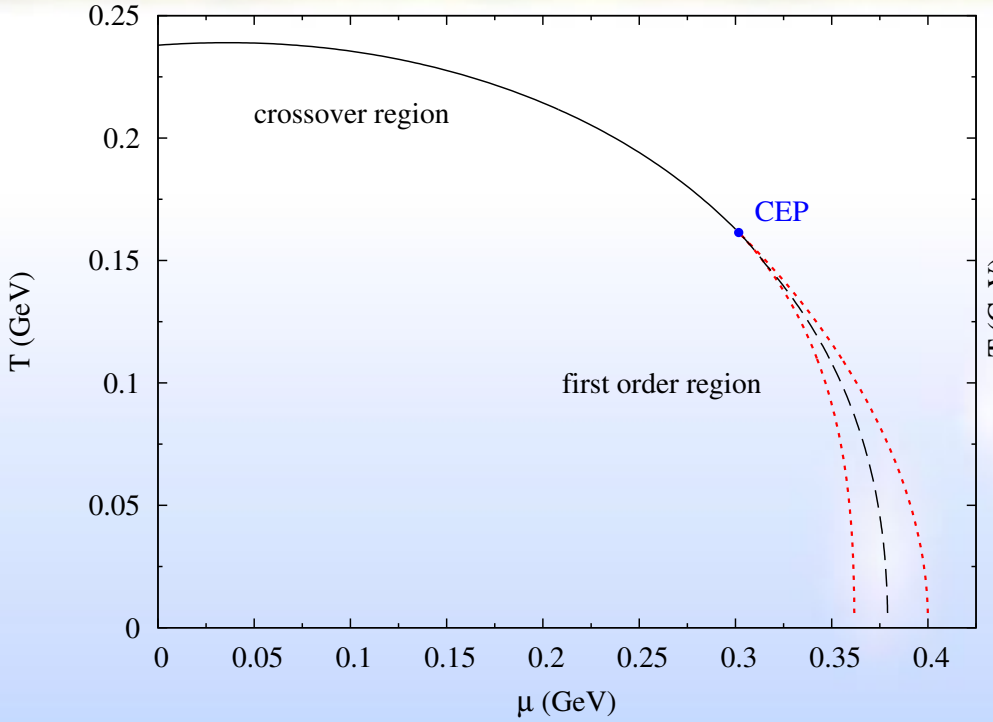

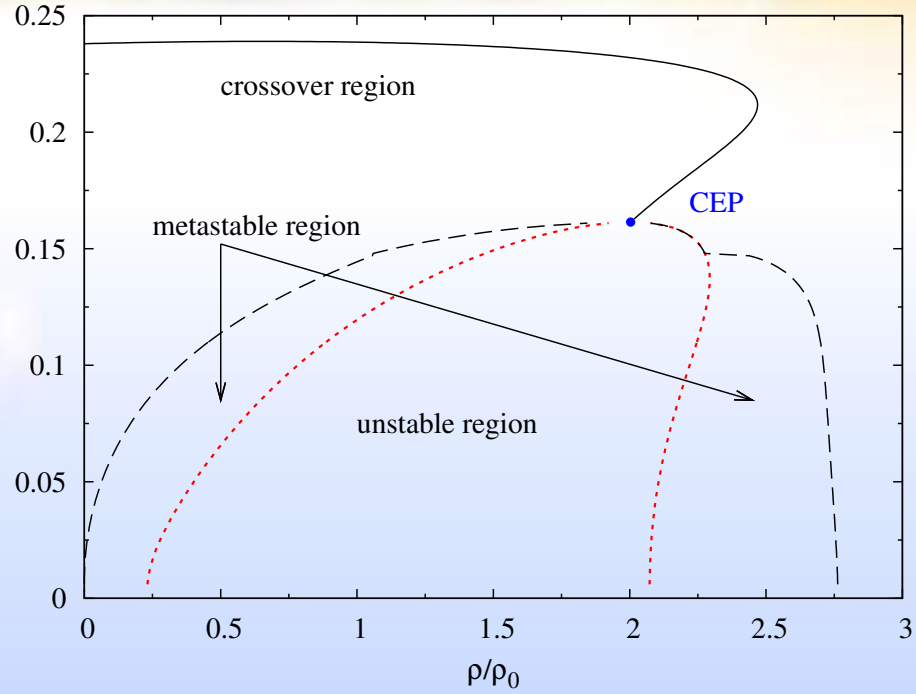

Left: (T, μ) phase diagram studying the transition in the condensate. CEP: ($\mu = 0.302$ GeV, $T = 0.161$GeV)
Right: (T, ρ) phase diagram. CEP: ($\rho = 2.00\rho_0$, $T = 0.161$ GeV).

Density: $\rho = 2N_cN_f \int_\Lambda \frac{d^3p}{(2\pi)^3}(f_\Phi^+(E_p) - f_\Phi^-(E_p))$

Third law of thermodynamics satisfied (parameter: Buballa)

Chiral and deconfinement crossover entanglement

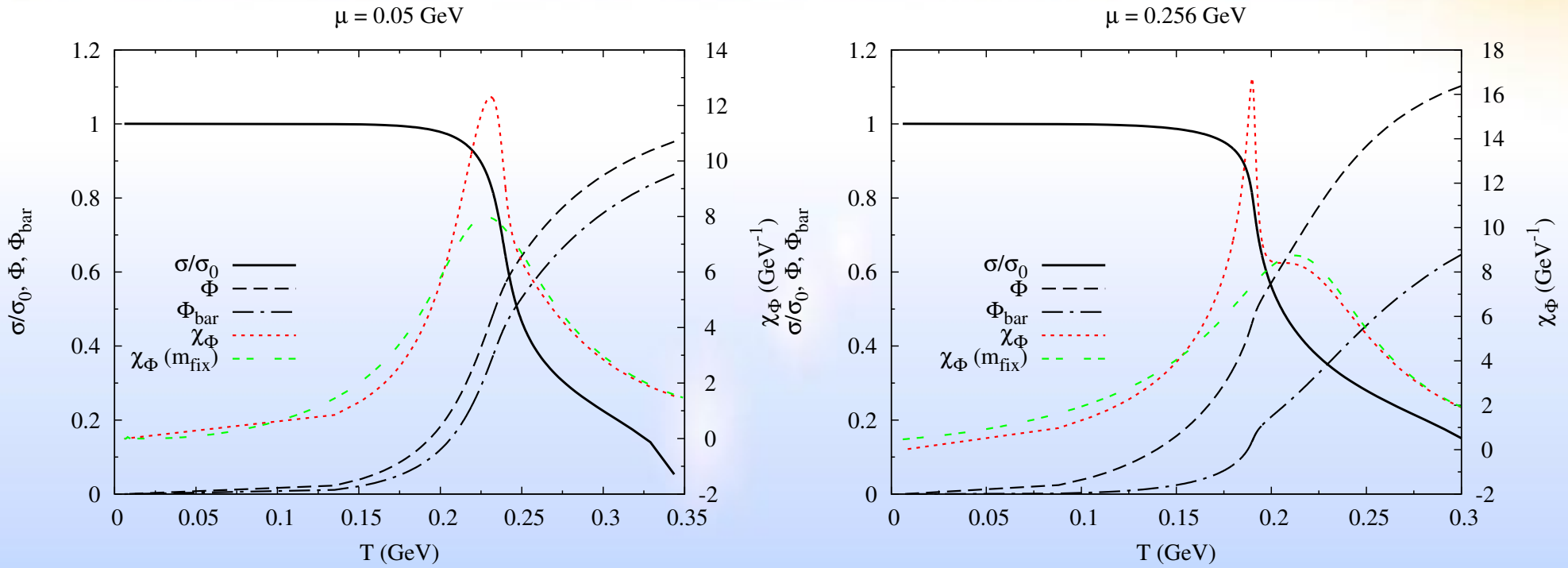

Left: Crossover zone ; red: deconfinement susceptibility ; green: susceptibility with m_{fix} for seeing the deconfinement transition entanglement.
Right: Crossover zone, near the critical end point ; red: deconfinement susceptibility ; green: susceptibility with m_{fix}.

The small influence of the mass on Φ allows to desentangle chiral and deconfinement transition.

High chemical potential region

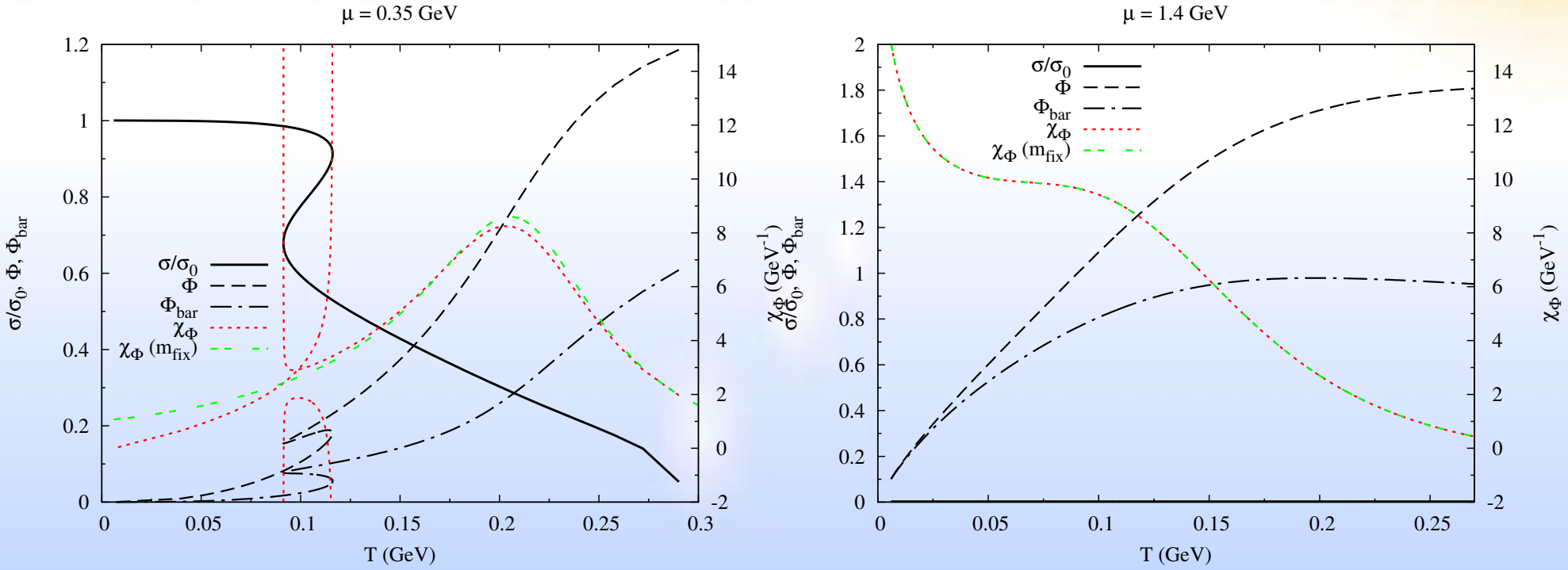

Left: Metastable zone ; red: deconfinement susceptibility ; green: susceptibility with m_{fix}.
Right: Zone where the chiral symmetry is restored ; there is no more a minimum of the deconfinement susceptibility.

Evolution of the deconfinement susceptibility

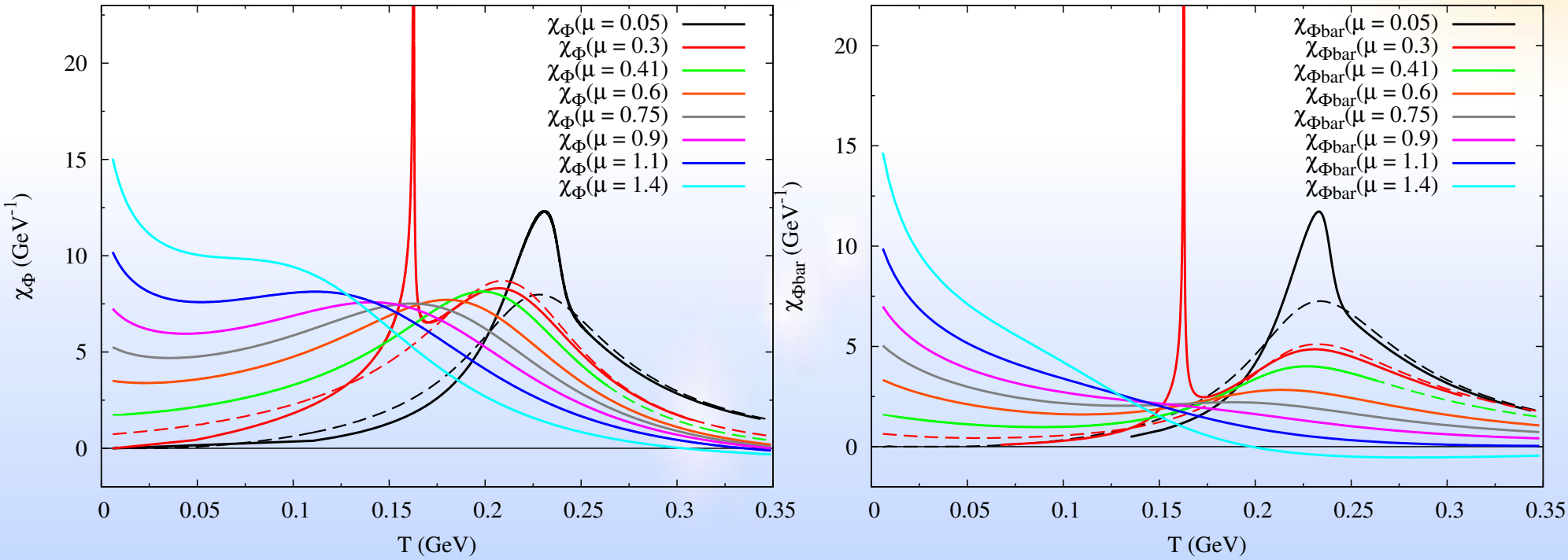

Left: Φ-susceptibility for different values of μ. The solid lines represent χ_Φ calculated with the Hartree mass, the dashed lines χ_Φ calculated with the constant mass (mean value between the mass at $(T = 0,\ \mu)$ and m_0). From the green line, increasing μ, we cannot see the dashed lines because χ_Φ is the same if we take a constant mass or the Hartree mass; actually in this region there is no more a chiral transition.
Right: $\bar{\Phi}$-susceptibility for different values of μ.

Phase diagram

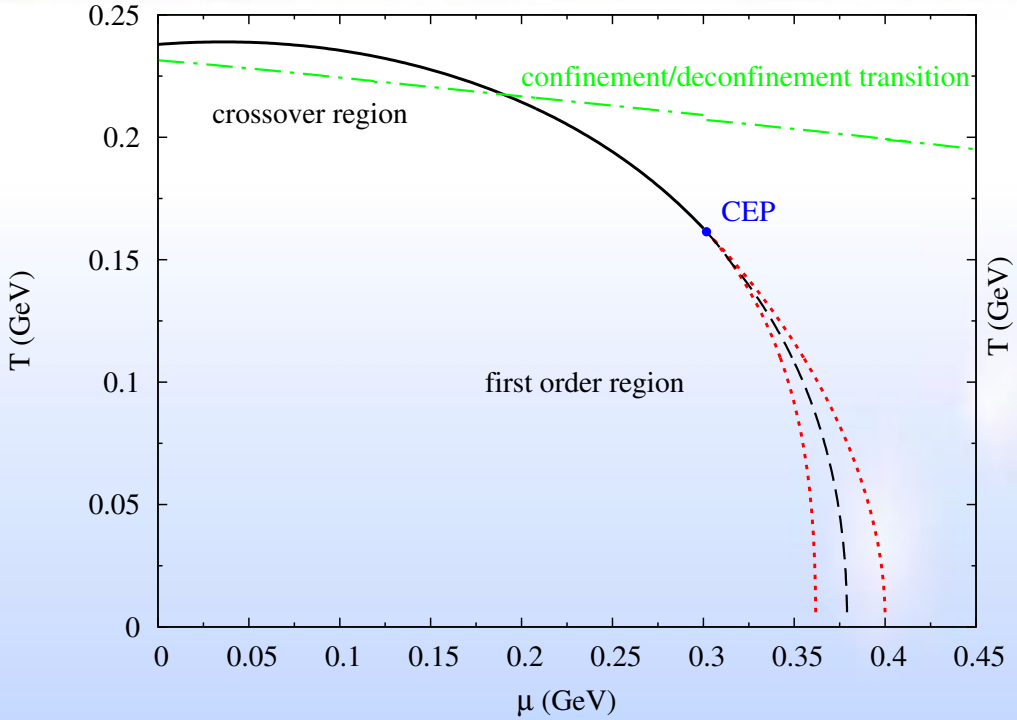

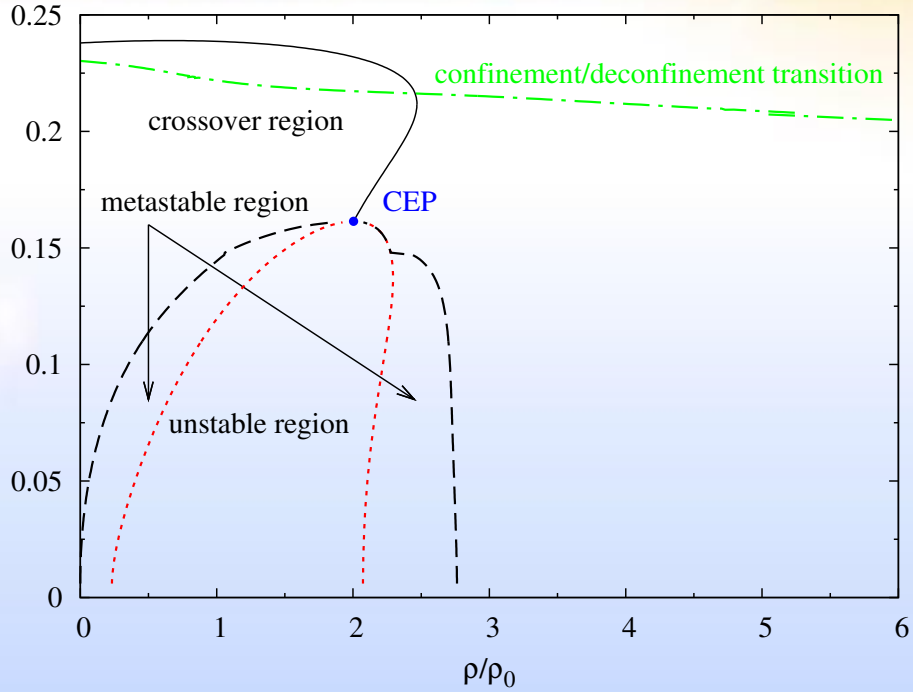

Phase diagram for Φ: the green line is the crossover point for Φ (i.e. $Max(d\Phi/dT)$).

Extended phase diagram

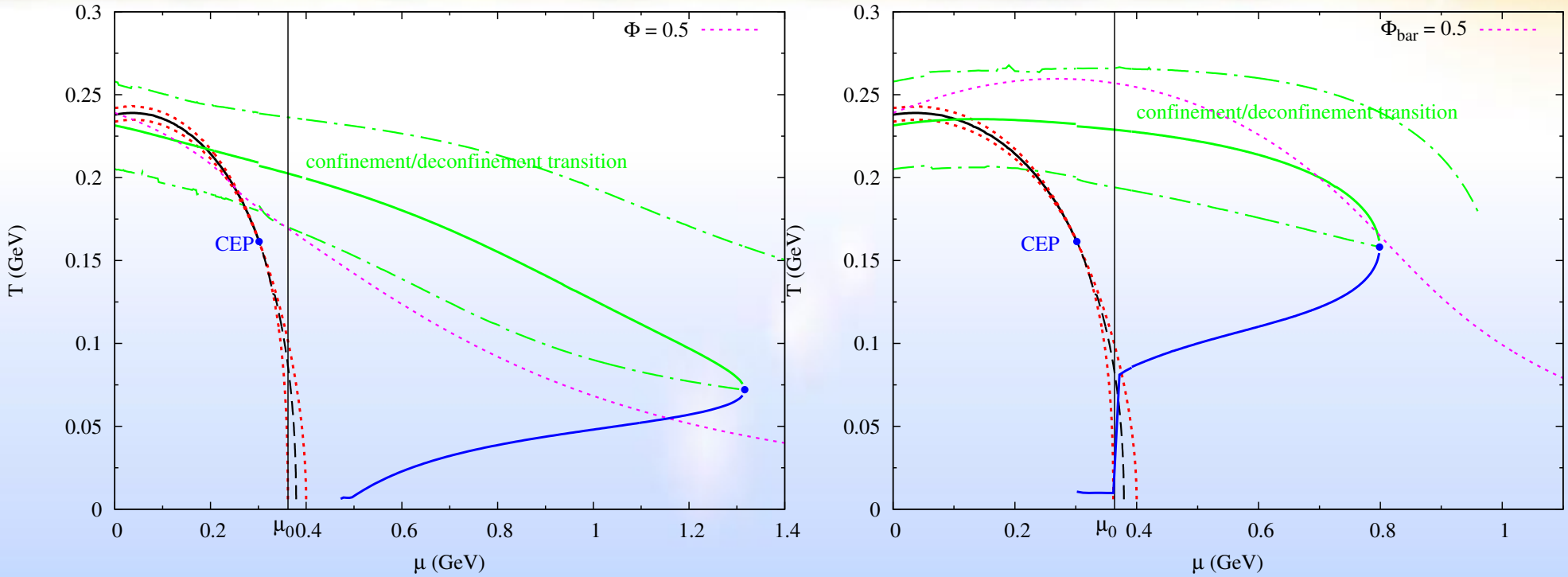

Left: Phase diagram for Φ: the green solid line is the crossover point for Φ ($Max(d\Phi/dT)$) ; the green dashed lines are the limits of the crossover zone (Max and Min of $d^2\Phi/dT^2$). For high densities we always are in the deconfined phase, except for $T = 0$, so the Φ-susceptibility approaches no more to zero, and so the blue line represents the minimum of the Φ-susceptibility that is produced from this fact. From the blue point it is no more possible to distinguish the maximum of the Φ-susceptibility because we are almost totally in the deconfinement phase, except for $T = 0$. The line at μ_0 is the point beyond which χ_Φ doesn't approach zero. The violet line is the point where $\Phi = 0.5$.
Right: Phase diagram for $\bar{\Phi}$

Part III: the SU(3) phase diagram and the role of strangeness

Order parameters evolution

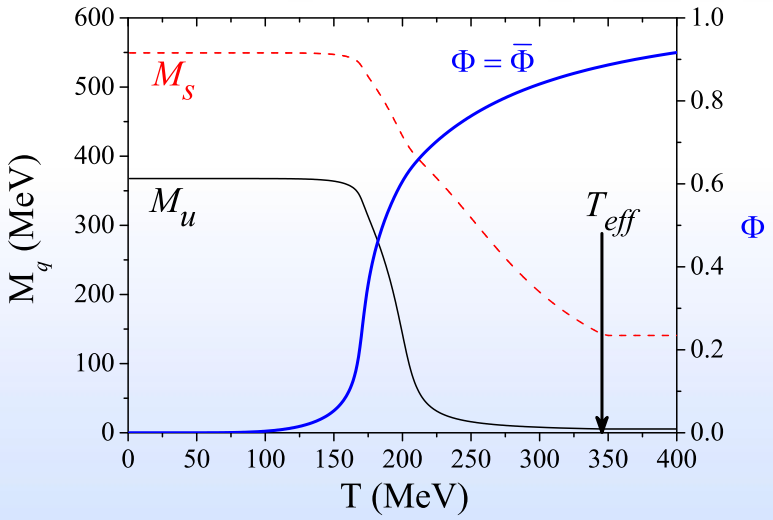

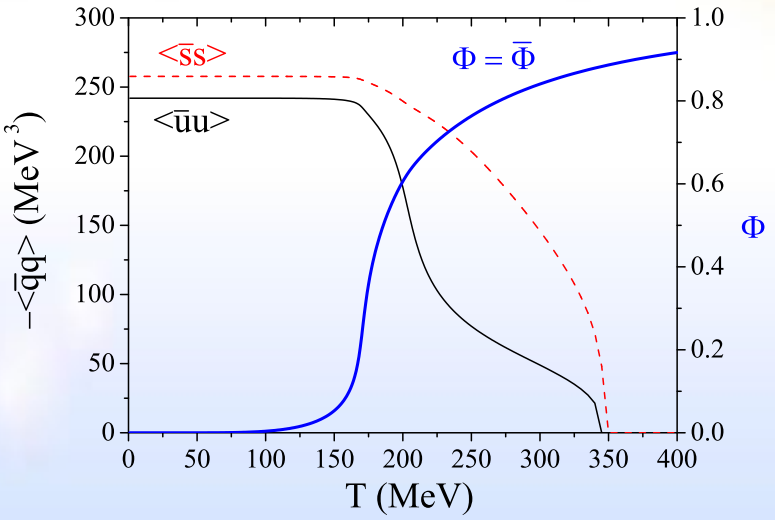

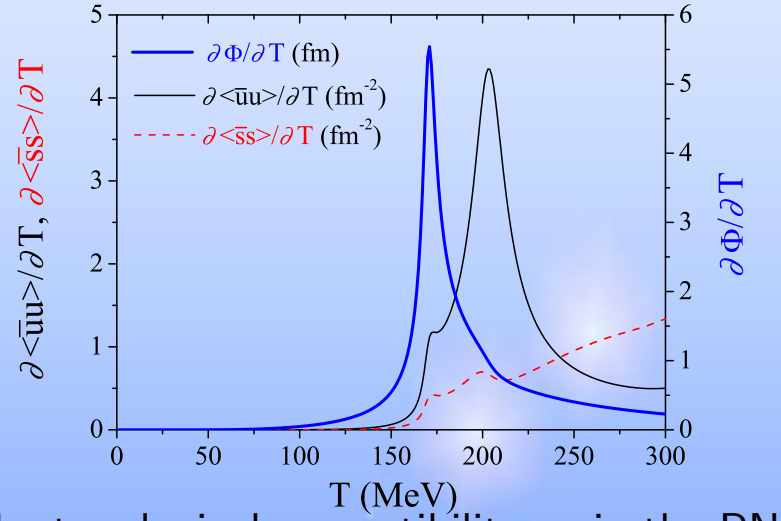

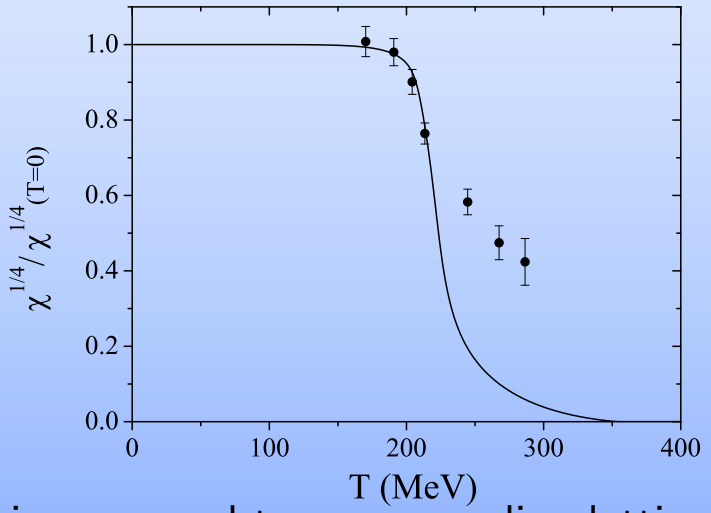

The topological susceptibility, χ in the PNJL model is compared to corresponding lattice results taken from Alles et al. (Nucl. Phys. B494, 281, 1997) ; Inflexion points of the strange and non-strange quark condensates are close (slightly separated from the one of Φ).

Thermodynamic Quantities (p,s and ε) at $\mu = 0$

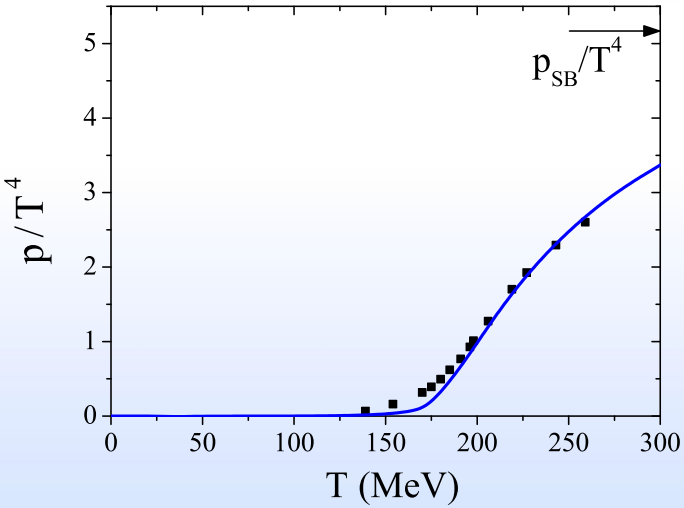

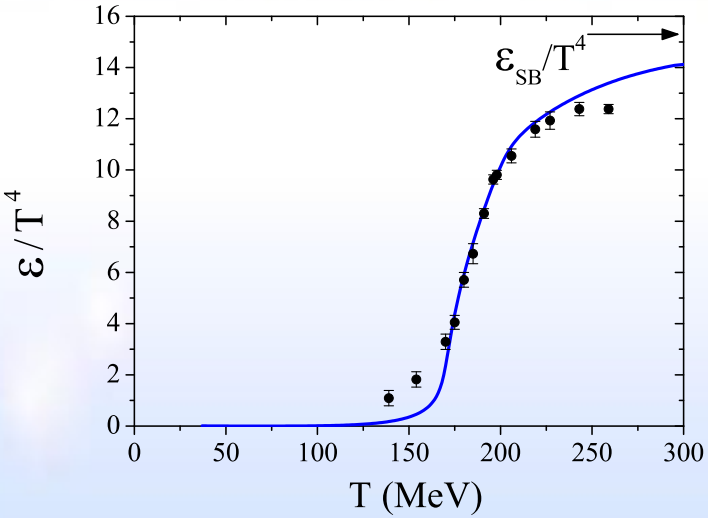

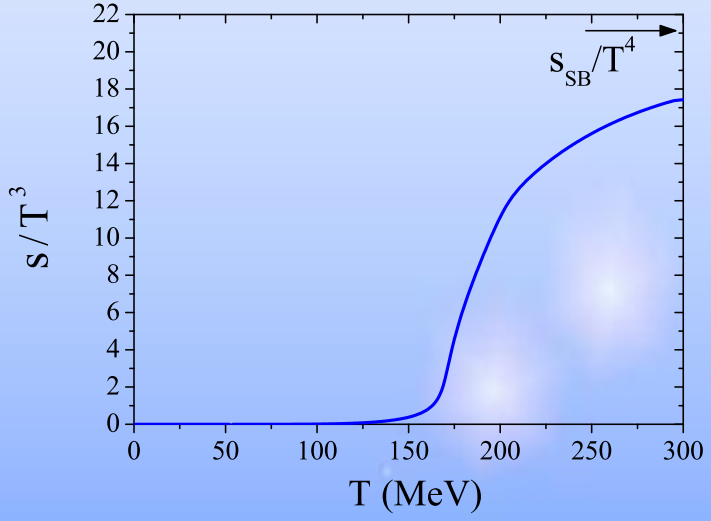

Asymptotically, the QCD pressure for N_f massless quarks and $(N_c^2 - 1)$ massless gluons is given $(\mu_B = 0)$ by:

$$\frac{p_{SB}}{T^4} = (N_c^2 - 1)\,\frac{\pi^2}{45} + N_c\,N_f\,\frac{7\,\pi^2}{180},$$

where the first term denotes the gluonic contribution and the second term the fermionic one.

Data: Cheng et al. (Phys. Rev. D81, 054504, 2009). The pressure reaches 66% of the strength of the Stefan-Boltzmann value at $T = 300$ MeV, a value which attains 85% at $T = 400$ MeV.

Phase Transition at Zero Temperature

First order phase transition $\mu^{cr} = 361.7$ MeV.

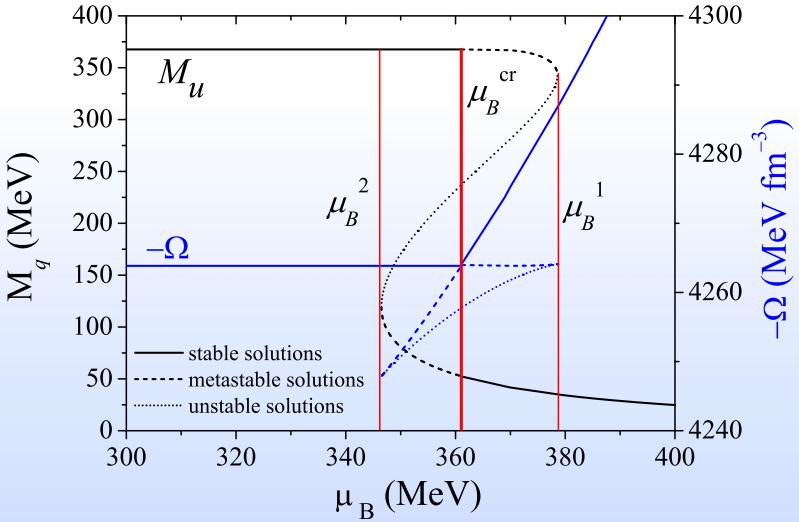

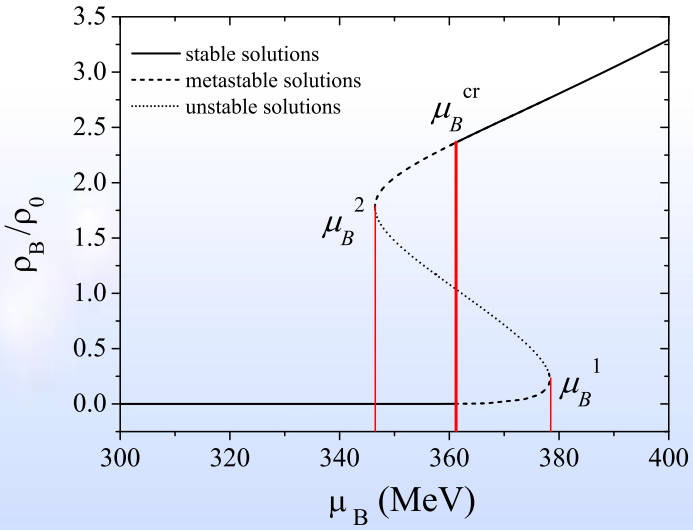

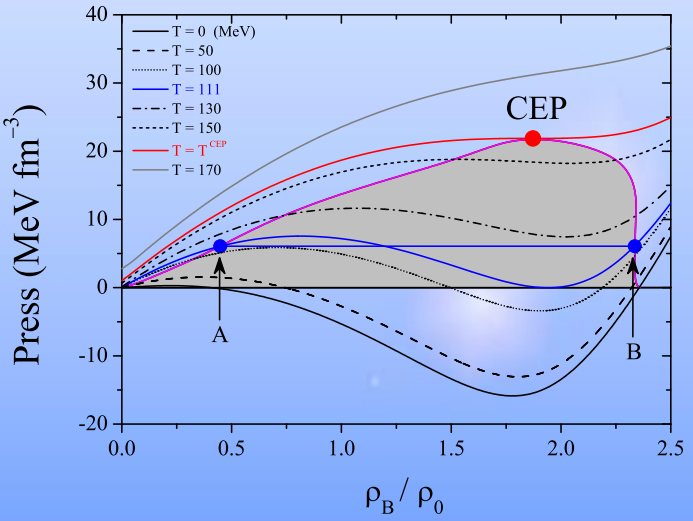

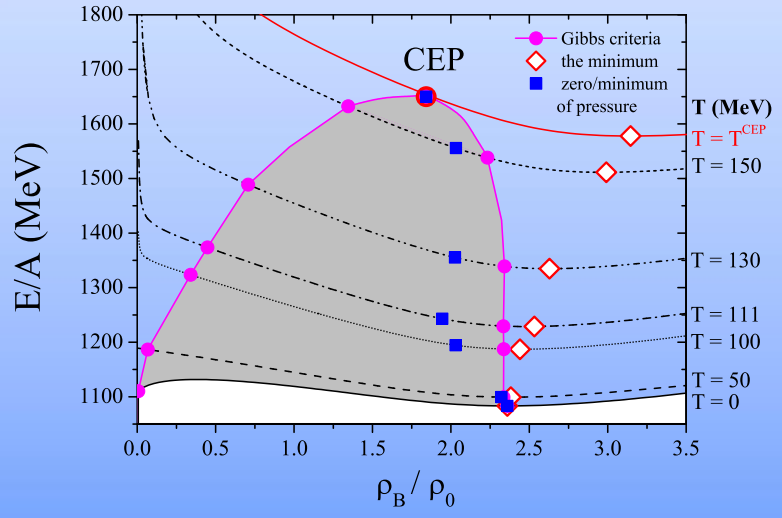

Phase Diagram and the Location of the Critical End Point

Location of the CEP: $T^{CEP} = 155.80$ MeV and $\rho_B^{CEP} = 1.87\rho_0$ ($\mu^{CEP} = 290.67$ MeV).

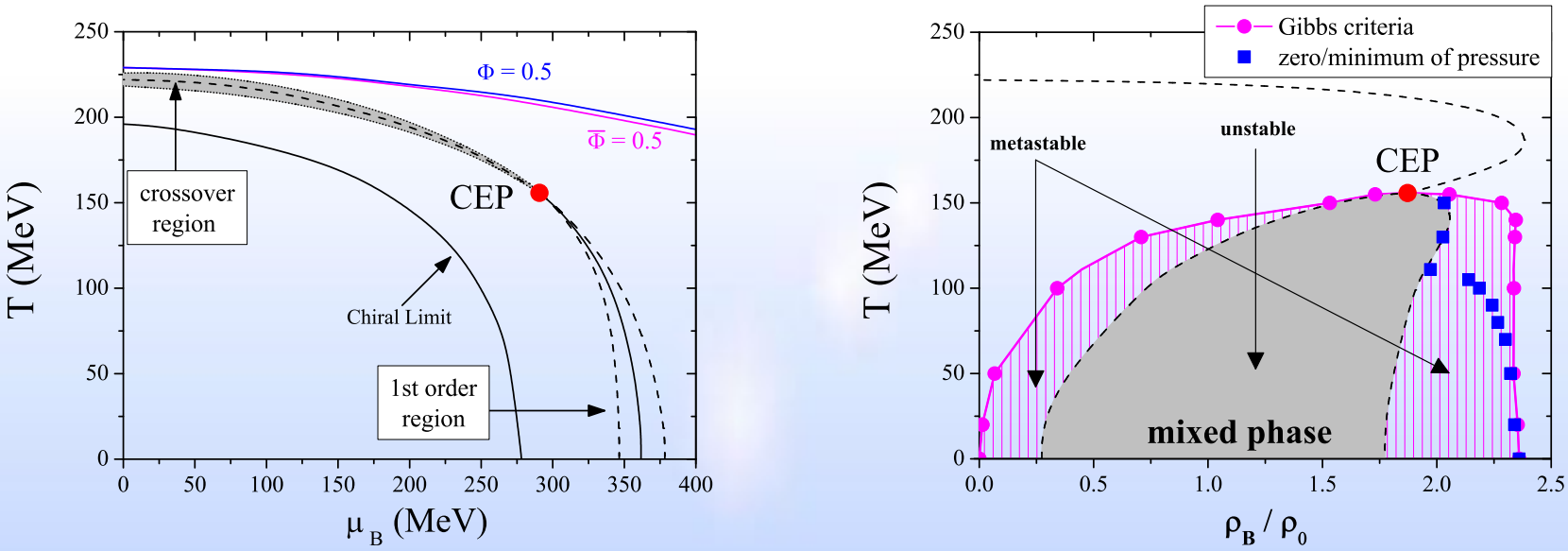

Phase diagram in the SU(3) PNJL model. The left (right) part corresponds to the $T - \mu_B$ ($T - \rho_B$) plane. Solid (dashed) line shows the location of the first order (crossover) transition. The dashed lines shows the location of the spinodal boundaries of the two phase transitions (shown by shading in the right plot).

Chiral and deconfinement transition

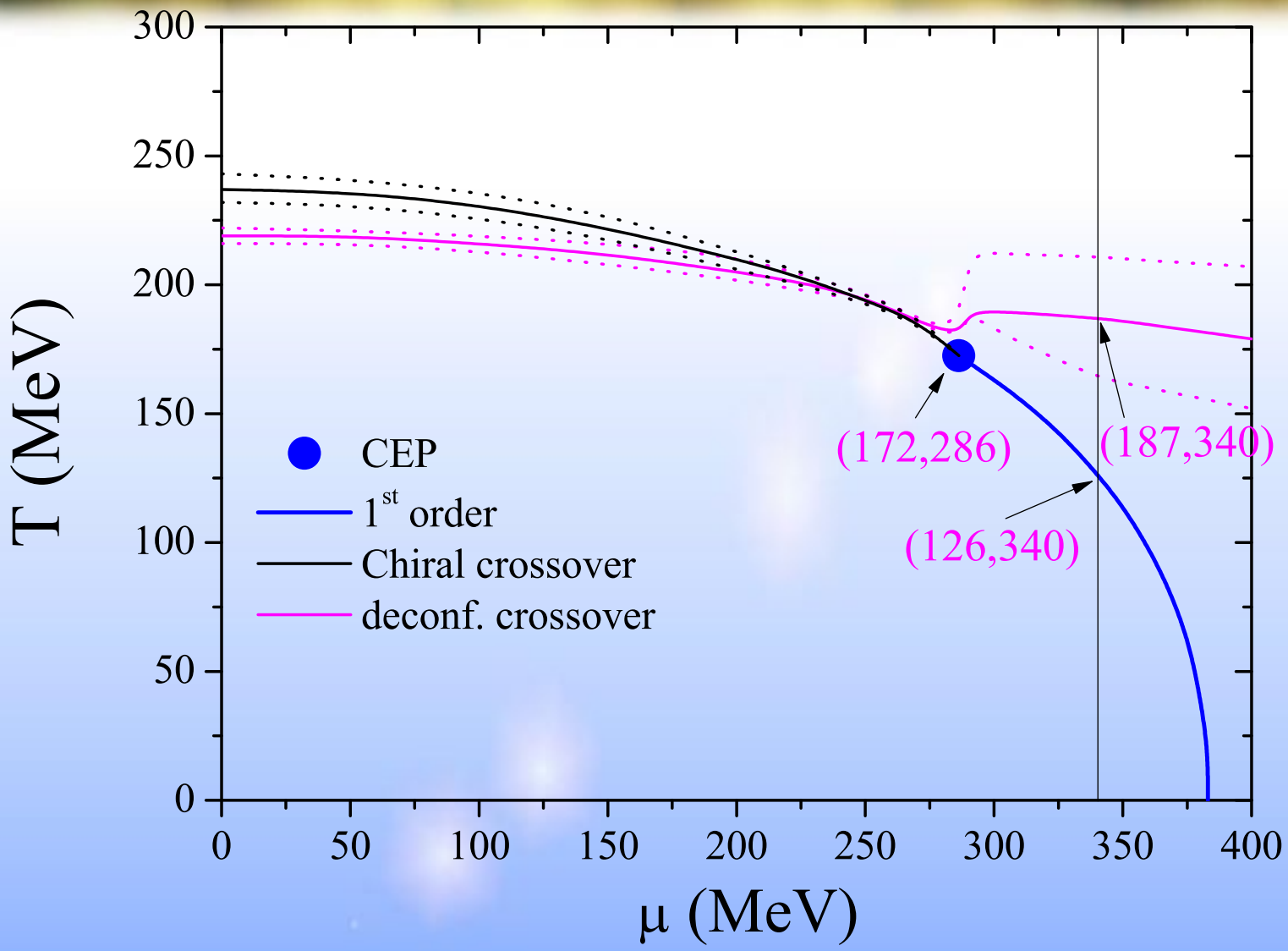

Opening of a phase with chiral symmetry and statiscally confined at the CEP

Nernst Principle and Isentropic Trajectories

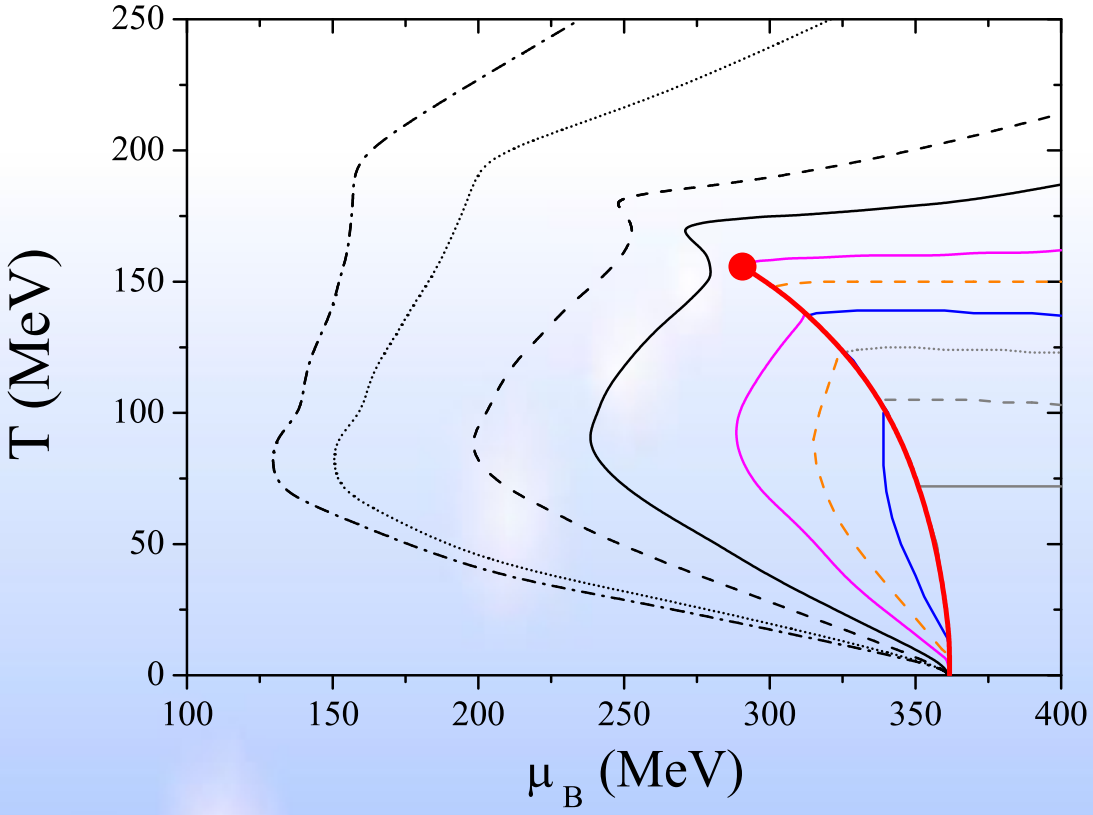

Isentropic trajectories in the (T, μ_B) plane. The following values of the entropy per baryon number have been considered: $s/\rho_B = 1,\ 2,\ 3,\ 4,\ 5,\ 6,\ 8,\ 10,\ 15,\ 20$ (anticlockwise direction).

Effects of Strangeness and Anomaly on the Critical End Point

Location of the CEP with physical mass: $m_u = m_d = 5.5$ MeV, $m_s = 140.7$ MeV $T^{CEP} = 155.80$ MeV and $\mu^{CEP} = 290.67$ MeV ($\rho_B^{CEP} = 1.87\rho_0$) ;

Chiral limit:

$\rightarrow m_u = m_d = m_s = 0 \Rightarrow$ no TCP: chiral symmetry is restored via a first order transition for all baryonic chemical potentials and temperatures

$\rightarrow$ in the light sector: $m_u = m_d$, $m_s \neq 0 \Rightarrow$ TCP

$\Rightarrow$ Both situations expected from universality argument (second order for $N_f = 2$ and first order for $N_f \geq 3$, Pisarski, 1983).

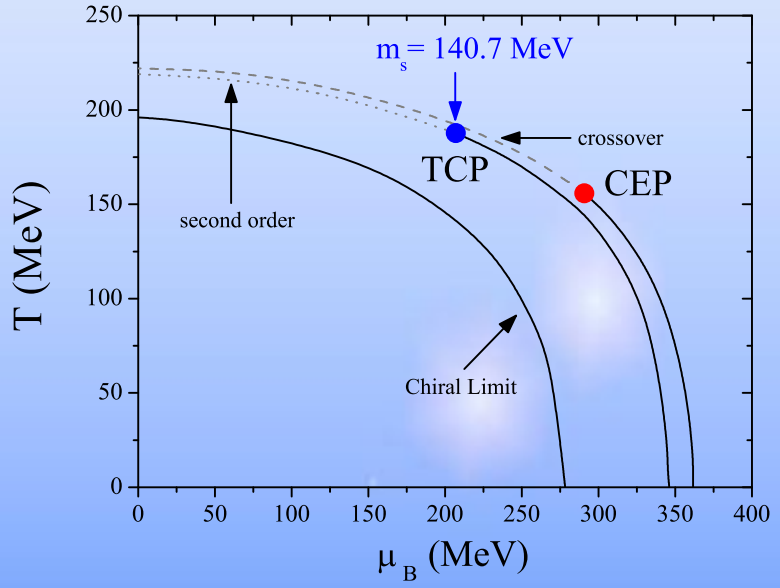

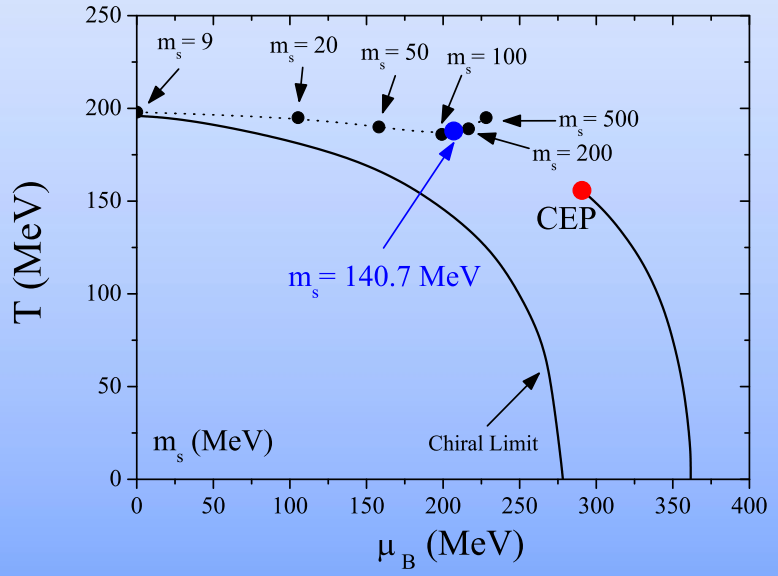

Role of the Anomaly Strength in the Location of the CEP

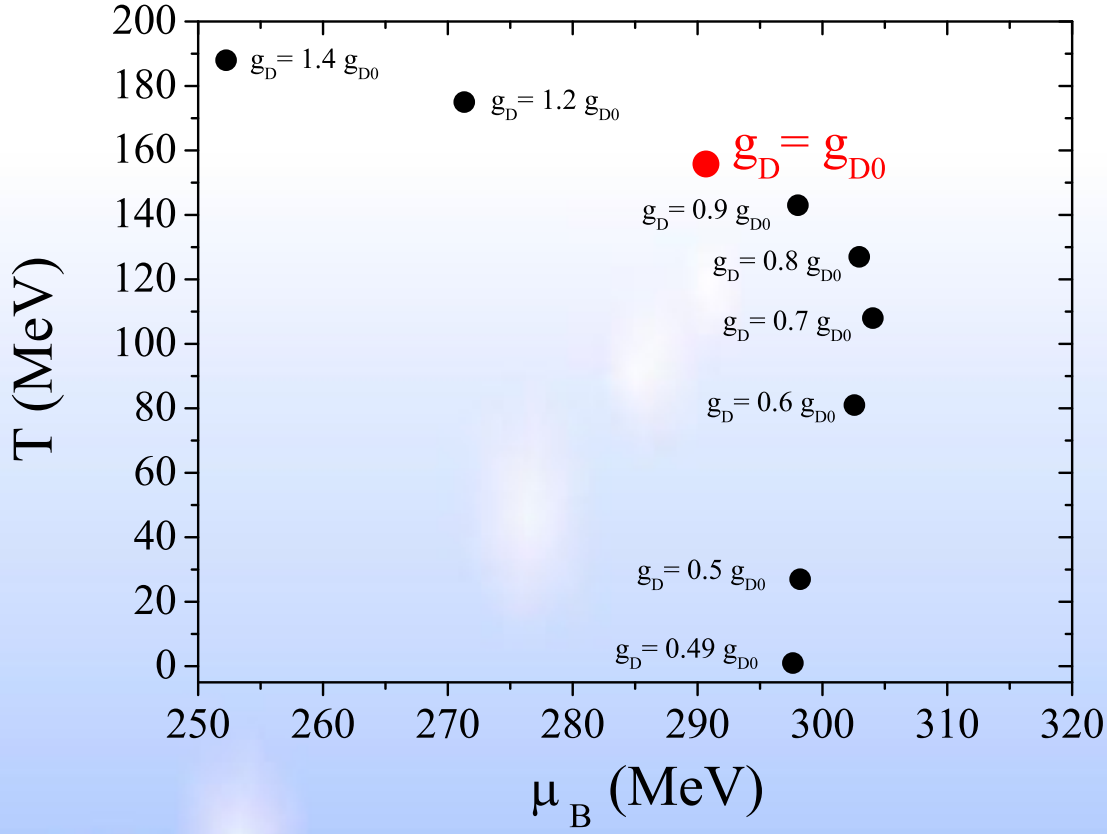

Dependence of the location of the CEP on the strength of the 't Hooft coupling constant g_D.

⇒ **Importance of the strangeness and anomaly for the CEP properties**

Susceptibilities and Critical Behavior in the Vicinity of the CEP

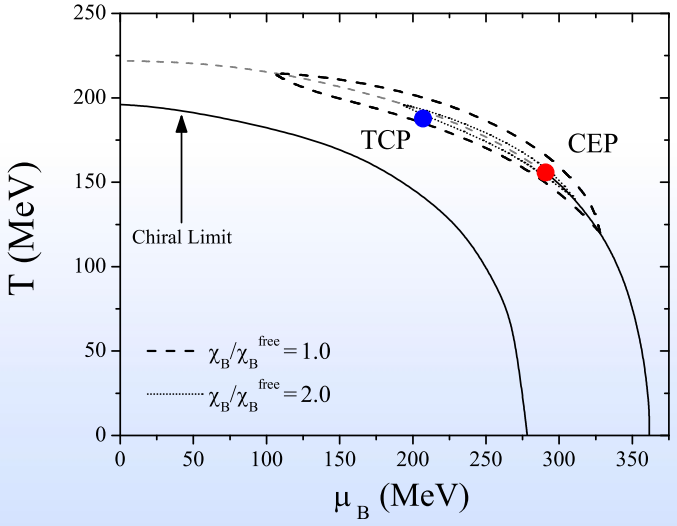

Phase diagram: the size of the critical region is plotted for $\chi_B/\chi_B^{free} = 1(2)$;
TCP - CEP entanglement: critical exponent goes from $1/2$ to $2/3$ when one approaches the CEP.
Left panel: Baryon number susceptibility as functions of μ_B for different temperatures around the CEP: $T^{CEP} = 155.80$ MeV and $T = T^{CEP} \pm 10$ MeV. Right panel: Specific heat as a function of T for different values of μ_B around the CEP: $\mu_B^{CEP} = 290.67$ MeV and $\mu_B = \mu_B^{CEP} \pm 10$ MeV.

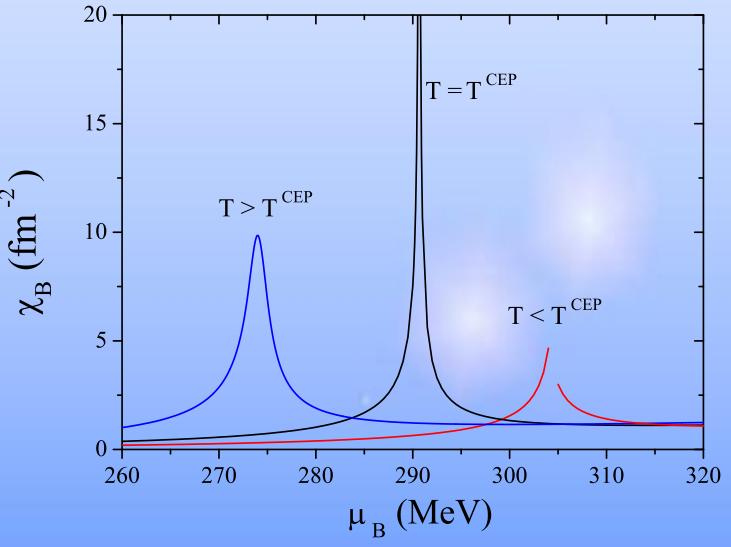

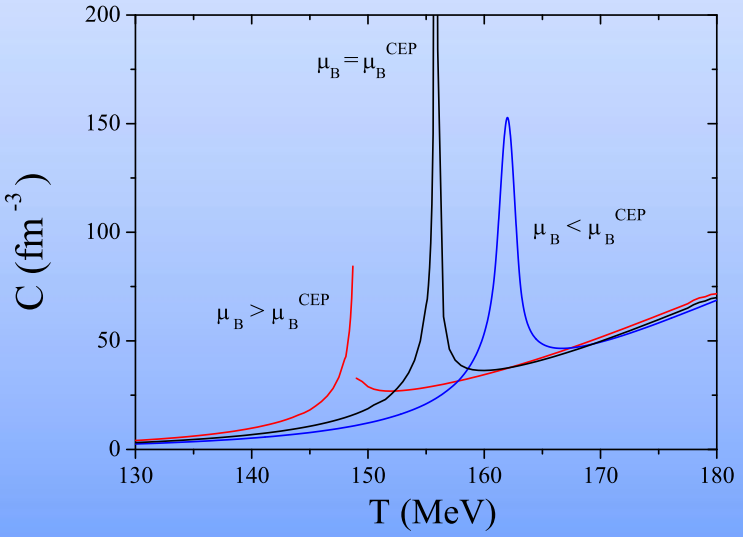

Conclusions

- The PNJL reproduces well at the mean field level the lattice calculations.
- PNJL calculations can be directly deduced from NJL ones (not only for one loop calculation, but to all orders) by a redefinition of the usual Fermi – Dirac distribution function.
- PNJL results does not destroy the important features like chiral restauration, Goldstone character of the pion, etc.
- The introduction of gluons in NJL via a background temporal gauge field embedded in the Polyakov loop add some statistical confinement to the NJL model. No mechanism for true confinement in PNJL ; yet The results are improved in the right direction (e.g. quarks more "bounded" in meson below T_c and less bound above T_c) compared to NJL.
- PNJL is a pertinent model to discuss confinement / deconfinement properties.

- Elongation of the critical region in the PNJL model.
- Influence of the strange sector on the critical behavior essential (existence/position of the CEP).
- Effects of the TCP on the CEP are seen.
- The sets of parameters used is compatible with the formation of stable droplets at zero temperature, insuring the Nernst principle.
- The regularization procedure by allowing high momentum quark states, is essential to obtain the required increase of extensive thermodynamic quantities, insuring the convergence to the Stefan–Boltzmann (SB) limit of QCD. In this context the gluonic degrees of freedom also play a special role.